Probabilistic Modeling of Negative-Sequence Current in Three-Phase Power Systems with Statistically Unbalanced Phases

DIEGO BELLAN
Department of Electronics, Information and Bioengineering,
Politecnico di Milano,
Piazza Leonardo da Vinci 32, 20133 Milan,
ITALY

Abstract: - In this work the parameters of an unbalanced three-phase component, such as a load or a transmission line, are described as random variables with known statistical properties. It is well-known that phase unbalancing leads to injected current in the negative-sequence circuit producing propagation of voltage unbalance and malfunctioning of power system components. In this paper, the injected current is described in probabilistic terms as a function of the statistical properties of the component unbalancing. In particular, approximate expressions for the probability density function, the mean value, and the variance of the injected current are derived in closed form and numerically validated.

Key-Words: - Asymmetrical three-phase systems, negative sequence current, probabilistic models, statistical analysis, unbalanced phases, voltage unbalance.

Received: September 19, 2021. Revised: September 14, 2022. Accepted: October 18, 2022. Published: November 11, 2022.

1 Introduction

Three-phase power systems under steady-state conditions are commonly analyzed by resorting to the well-known Symmetrical Component Transformation (SCT), [1], [2], [3], [4]. The main advantage of the SCT consists in the derivation of three uncoupled circuits named positive/negative/zero-sequence circuits, with transformed voltages/currents named positive/negative/zero-sequence voltages/currents.

This result can be achieved because the SCT is able to decouple the originally coupled equations describing the given three-phase system, [4]. The main assumption underlying the effectiveness of the SCT is that the three phases are symmetrical, i.e., the passive part of the three phases is balanced (e.g., equal self-impedances, and equal mutual impedances). This is an ideal condition that can be only approximated in real-world applications by 1) using transposition of transmission lines, 2) distributing the loads uniformly between the three phases.

In modern power systems, however, balancing the three phases is becoming more and more complicated, especially because of the increasing number of large single-phase loads. The main consequence of unbalanced phases is that the SCT leads to coupled sequence circuits. Thus, the positive-sequence circuit injects current in both the negative and the zero-sequence circuits, [5]. This is a critical point because negative and zero-sequence currents can easily cause malfunctioning of many electrical apparatus connected to the power system, [6]. For this reason, many research contributions can be found in the literature about modeling and calculation of voltages and currents due to unbalanced phases (i.e., asymmetrical lines and loads), [7], [8], [9], [10], [11], [12], [13], [14], [15], [16], [17], [18], [19]. Such contributions, however, assume a deterministic knowledge of system asymmetries. In many practical conditions it would be more useful to consider the statistical uncertainty of line/load parameters, [20].

In this paper, it is assumed that unbalancing of the three phases of a given component is described in statistical terms. More specifically, it is assumed that the parameters of a three-phase component (i.e., line or load) can be treated as random variables with a given statistical distribution. Such an unbalanced component is responsible for injection of current in the negative-sequence circuit (the zero-sequence circuit is not involved since the analysis is limited to three-wire systems). The injected current, as a function of the unbalanced component parameters, is a random variable as well. The main objective of the paper is providing the probabilistic description of the injected negative-sequence current as a function of the statistical properties of the unbalanced component parameters. In particular, approximate analytical expressions for the

probability density function, the mean value, and the variance of the injected current are derived in closed form.

The paper is organized as follows. In Section 2 an approximate expression for the negative-sequence current is derived as a function of the parameters of an unbalanced three-phase component. In Section 3 the probabilistic modeling of the injected current is derived in closed form by assuming Gaussian distribution of the unbalanced component parameters. In Section 4 the analytical results are validated by means of numerical simulations.

2 Negative-Sequence Current due to Unbalanced Phases

Let us consider a basic three-phase radial network consisting of a voltage source, transmission line, and load (see Fig. 1). Under sinusoidal steady-state conditions, the system can be readily analyzed by means of the well-known SCT. In fact, under the crucial assumption of balanced (i.e., symmetrical) phases, the SCT leads to three uncoupled circuits in the transformed variables, i.e., the so-called positive/negative/zero-sequence circuits with corresponding sequence voltages and currents. Each sequence circuit can be solved independently from the other circuits through standard techniques. Finally, the inverse SCT can be applied to the sequence-domain solution to obtain the solution in the original *a,b,c*, domain.

The procedure outlined above is effective under the crucial assumption of balanced phases, i.e., a passive three-phase component characterized by a symmetrical matrix with equal elements on the main diagonal, and equal off-diagonal elements. For example, by considering a three-phase component characterized by an impedance matrix, the three self-impedances must be equal to each other, and the three mutual impedances must be equal to each other. In case this crucial assumption is not met, the SCT leads to coupled sequence circuits instead of uncoupled. By assuming that the system depicted in Fig. 1 is a three-wire three-phase system, only the positive and the negative-sequence circuits are involved in the analysis since the zero-sequence circuit is open. Therefore, an unbalanced three-phase component in Fig. 1 results in coupled positive and the negative-sequence circuits (Fig. 2).

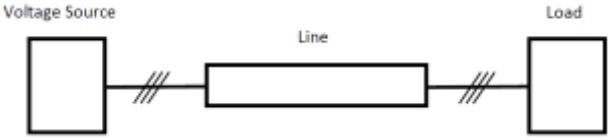

Fig. 1: Three-phase radial network.

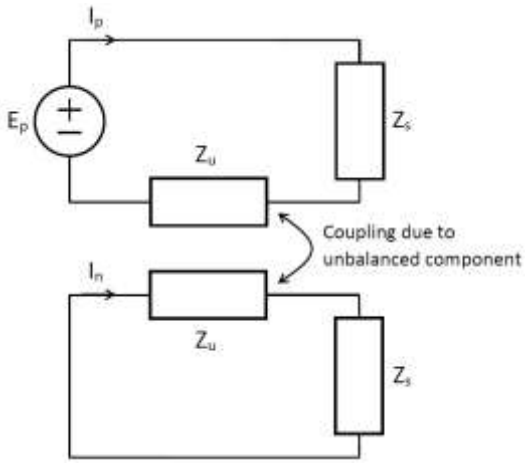

Fig. 2: Positive and negative-sequence circuits. Balanced three-phase components result in the total sequence impedance Zs. Coupling is due to the unbalanced three-phase component with impedance matrix Zu.

In general terms, the solution of the circuit in Fig. 2 requires the evaluation of coupled equations. Therefore, in this case the SCT does not lead to a simpler solution with respect to the original problem in the *a,b,c* variables. However, in [19] it was shown that, under proper and general assumptions, the circuit coupling in Fig. 2 can be regarded as a weak coupling. It means that an approximate approach can be adopted where the feedback from the negative to the positive-sequence circuit can be neglected. Thus, the positive-sequence current can be evaluated by neglecting circuit coupling, whereas the negative-sequence current can be evaluated by considering a simple controlled source taking into account the circuit coupling. This approximate approach can be easily explained by observing that, under ideal conditions, the negative-sequence current is zero. Thus, a component unbalance can be regarded as a perturbation of an ideal system where only the positive-sequence current is flowing. The unbalanced three-phase component injects current in the negative-sequence circuit. As a result, the negative-sequence current is normally a small fraction of the positive-sequence current. This point explains the above mentioned weak-coupling assumption.

More specifically, let us consider an unbalanced three-phase component characterized by the following impedance matrix:

$$\boldsymbol{Z}_u = \begin{bmatrix} Z_a & 0 & 0 \\ 0 & Z_b & 0 \\ 0 & 0 & Z_c \end{bmatrix} \quad (1)$$

By denoting with Z the balanced value of the impedances, we can write:

$$\boldsymbol{Z}_u = \begin{bmatrix} Z & 0 & 0 \\ 0 & Z & 0 \\ 0 & 0 & Z \end{bmatrix} + \begin{bmatrix} \delta_a & 0 & 0 \\ 0 & \delta_b & 0 \\ 0 & 0 & \delta_c \end{bmatrix} = \boldsymbol{Z} + \boldsymbol{\delta Z} \quad (2)$$

By using the SCT in (2), the balanced matrix $\boldsymbol{Z}$ remains unchanged, whereas the deviation $\boldsymbol{\delta Z}$ in the sequence domain is given by:

$$\boldsymbol{\delta Z}_s = \boldsymbol{S} \begin{bmatrix} \delta_a & 0 & 0 \\ 0 & \delta_b & 0 \\ 0 & 0 & \delta_c \end{bmatrix} \boldsymbol{S}^{-1} = \begin{bmatrix} \delta_m & \delta_n & \delta_p \\ \delta_p & \delta_m & \delta_n \\ \delta_n & \delta_p & \delta_m \end{bmatrix} \quad (3)$$

where:

$$\delta_m = \frac{1}{3}(\delta_a + \delta_b + \delta_c) \quad (4)$$

$$\delta_p = \frac{1}{3}(\delta_a + \alpha\delta_b + \alpha^2\delta_c) \quad (5)$$

$$\delta_n = \frac{1}{3}(\delta_a + \alpha^2\delta_b + \alpha\delta_c) \quad (6)$$

and the SCT matrix $\boldsymbol{S}$ in rational form is defined as:

$$\boldsymbol{S} = \frac{1}{\sqrt{3}} \begin{bmatrix} 1 & \alpha & \alpha^2 \\ 1 & \alpha^2 & \alpha \\ 1 & 1 & 1 \end{bmatrix} \quad (7)$$

where $\alpha = e^{j2\pi/3}$.
Since we assume the system in Fig. 2 as a three-wire system, only the positive and negative-sequence circuits must be considered. Thus, circuit coupling between those sequence circuits is described by the first two rows and columns of the matrix in (3):

$$\begin{bmatrix} V_p \\ V_n \end{bmatrix} = \begin{bmatrix} Z & 0 \\ 0 & Z \end{bmatrix} \begin{bmatrix} I_p \\ I_n \end{bmatrix} + \begin{bmatrix} \delta_m & \delta_n \\ \delta_p & \delta_m \end{bmatrix} \begin{bmatrix} I_p \\ I_n \end{bmatrix} \quad (8)$$

Notice that by assuming small impedance deviations, i.e.,

$$|\delta_a|, |\delta_b|, |\delta_c| \ll |Z| \quad (9)$$

the terms $\delta_m I_p$ and $\delta_m I_n$ in (9) can be neglected. Moreover, the above-mentioned approximate approach based on the assumption of weak coupling between the two sequence circuits allows neglecting the term $\delta_n I_n$ representing the feedback from the negative to the positive-sequence circuit. Thus, from (8) we obtain a voltage perturbation in the negative-sequence circuit given by:

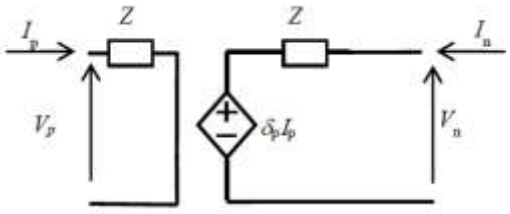

Fig. 3: Approximate equivalent circuit for the unbalanced component $\boldsymbol{Z}_u$. Unbalancing is represented by a current-controlled voltage source in the negative-sequence circuit.

$$\delta V_n \cong \delta_p I_p \quad (10)$$

Such perturbation can be represented as a current-controlled voltage source (see Fig. 3). The negative-sequence current is given by:

$$I_n = -\frac{\delta V_n}{Z_t} \cong -\frac{\delta_p I_p}{Z_t} \quad (11)$$

where Z_t is the total balanced impedance in the positive and negative-sequence circuits. Thus, the ratio between negative and positive-sequence currents is given by:

$$\beta = \left|\frac{I_n}{I_p}\right| \cong \left|\frac{\delta_p}{Z_t}\right| \quad (12)$$

The current ratio β given in (12) will be analyzed as a random variable in the next Section.

3 Probabilistic Modeling of Negative-Sequence Current

The negative-sequence current (normalized by the positive-sequence current) given by (12) can be regarded as a random variable when the impedance deviations $\delta_a, \delta_b, \delta_c$ of the unbalanced three-phase component are given in statistical terms. For the sake of simplicity, in this paper we assume real impedance deviations $\delta_a, \delta_b, \delta_c$ (i.e., we assume that only the resistive parts are deviating from the balanced value). Therefore, from (5) we obtain that (12) can be rewritten as:

$$\beta = \frac{1}{3|Z_t|}|\delta_a + \alpha\delta_b + \alpha^2\delta_c| =$$

$$= \frac{1}{|Z_t|}\sqrt{\frac{1}{9}\left(\delta_a - \frac{\delta_b+\delta_c}{2}\right)^2 + \frac{1}{12}(\delta_b - \delta_c)^2} \quad (13)$$

Therefore, β can be regarded as a function of the random variables $\delta_a, \delta_b, \delta_c$. In this Section the statistical properties of the random variable β will be derived as functions of the statistical properties of the uncorrelated random variables $\delta_a, \delta_b, \delta_c$. To this aim, we study the following transformation of random variables:

$$w = \sqrt{x^2 + y^2} \quad (14)$$

where:

$$x = \frac{1}{3}\left(\delta_a - \frac{\delta_b+\delta_c}{2}\right), \quad y = \frac{1}{2\sqrt{3}}(\delta_b - \delta_c) \quad (15)$$

Assuming $\delta_a, \delta_b, \delta_c$ with zero mean values, the random variables *x* and *y* are also unbiased, i.e., $\mu_x = \mu_y = 0$. The variances of *x* and *y* are given by:

$$\sigma_x^2 = \frac{1}{9}\left(\sigma_a^2 + \frac{\sigma_b^2+\sigma_c^2}{4}\right), \quad \sigma_y^2 = \frac{1}{12}\left(\sigma_b^2 + \sigma_c^2\right) \quad (16)$$

Notice that even in the case of $\delta_a, \delta_b, \delta_c$ with Gaussian distribution, the random variable *w* given by (14) is not a Rayleigh variable for two reasons. First, the two variances in (16), in general, are not equal. Second, since δ_b and δ_c are both involved in the definition of *x* and *y* in (15), the random variables *x* and *y*, in general, are correlated. The correlation coefficient r_{xy} can be readily evaluated, [21], [22], [23]:

$$r_{xy} = \frac{E\{xy\}-\mu_x\mu_y}{\sigma_x\sigma_y} = \frac{1-\left(\frac{\sigma_b}{\sigma_c}\right)^2}{1+\left(\frac{\sigma_b}{\sigma_c}\right)^2} \frac{1}{\sqrt{1+4\frac{\left(\frac{\sigma_a}{\sigma_c}\right)^2}{1+\left(\frac{\sigma_b}{\sigma_c}\right)^2}}} \quad (17)$$

From (17) it can be observed that in the special case $\sigma_b = \sigma_c$ the random variables *x* and *y* are uncorrelated. In this case, the random variable *w* in (14) can be approximated by a Rayleigh random variable with parameter σ^2 given by the average value of the variances σ_x^2 and σ_y^2, i.e.,

$$f_w(w) \cong \frac{w}{\sigma^2} e^{-\frac{w^2}{2\sigma^2}} \quad (18)$$

where f_w is the probability density function (PDF) of *w*, and

$$\sigma^2 = \frac{1}{2}\left(\sigma_x^2 + \sigma_y^2\right) \quad (19)$$

In the general case, however, the random variables *x* and *y* are correlated, and the approximate PDF (18) cannot be used. In this case an approximate approach based on the Taylor expansion can be used to estimate the mean value and the variance of *w*, [24]. To this aim, in order to obtain simpler and consistent derivations, a further change of variables is used. By letting $u = x^2$ and $v = y^2$, from (14) we obtain:

$$w = \sqrt{u + v} \quad (20)$$

By assuming Gaussian distribution for the random variables $\delta_a, \delta_b, \delta_c$, the mean values and the variances of *u* and *v* are given by:

$$\mu_u = \sigma_x^2, \quad \sigma_u^2 = 2\sigma_x^4 \quad (21)$$

$$\mu_v = \sigma_y^2, \quad \sigma_v^2 = 2\sigma_y^4 \quad (22)$$

Notice again that, in general, the random variables *u* and *v* are correlated since δ_b and δ_c are both in the definition of *u* and *v*. Therefore, the evaluation of the correlation coefficient r_{uv} is required. After simple algebra we obtain:

$$r_{uv} = \frac{E\{uv\}-\mu_u\mu_v}{\sigma_u\sigma_v} = \left(\frac{1-\left(\frac{\sigma_b}{\sigma_c}\right)^2}{1+\left(\frac{\sigma_b}{\sigma_c}\right)^2}\right)^2 \frac{1}{1+4\frac{\left(\frac{\sigma_a}{\sigma_c}\right)^2}{1+\left(\frac{\sigma_b}{\sigma_c}\right)^2}} \quad (23)$$

The correlation coefficient r_{uv} is the square of r_{xy} because of the definition of *u* and *v* as the square of *x* and *y*, respectively. We can observe that r_{xy} keeps the information about the sign of the correlation, whereas r_{uv} is always positive. Also in this case we obtain $r_{uv} = 0$ when $\sigma_b = \sigma_c$.

The mean value and the variance of the random variable *w* can be estimated by resorting to the Taylor series expansion, [21], [22], [23], [24]:

$$\mu_w \cong \sqrt{\mu_u + \mu_v} + \\ + \frac{1}{2}\left(\frac{\partial^2 w}{\partial u^2}\sigma_u^2 + 2\frac{\partial^2 w}{\partial u\,\partial v} r_{uv}\sigma_u\sigma_v + \frac{\partial^2 w}{\partial v^2}\sigma_v^2\right) \quad (24)$$

$$\sigma_w^2 \cong \left(\frac{\partial w}{\partial u}\right)^2 \sigma_u^2 + \\ + 2\left(\frac{\partial w}{\partial u}\right)\left(\frac{\partial w}{\partial v}\right) r_{uv}\sigma_u\sigma_v + \left(\frac{\partial w}{\partial v}\right)^2 \sigma_v^2 \quad (25)$$

where the derivatives are evaluated at $u = \mu_u$ and $v = \mu_v$. Notice that if the same approach was used for *w* as a function of *x* and *y*, instead of *u* and *v*, all the derivatives in (24)-(25) were zero. This explains

the reason for the use of the variables *u* and *v*.
From (24)-(25) after simple algebra we obtain:

$$\mu_w \cong \sqrt{\sigma_x^2+\sigma_y^2} - \frac{\sigma_x^4+2r_{uv}\sigma_x^2\sigma_y^2+\sigma_y^4}{4\left(\sigma_x^2+\sigma_y^2\right)^{3/2}} \quad (26)$$

$$\sigma_w^2 \cong \frac{\sigma_x^4+2r_{uv}\sigma_x^2\sigma_y^2+\sigma_y^4}{2\left(\sigma_x^2+\sigma_y^2\right)} \quad (27)$$

where σ_x^2, σ_y^2, and r_{uv} are given by (16) and (23) as functions of $\sigma_a^2, \sigma_b^2, \sigma_c^2$.
Finally, it can be noticed that the above analytical results can be readily used for the original random variable β given in (13). In particular, the approximate PDF (18) becomes:

$$f_\beta(\beta) \cong |Z_t| \frac{\beta}{\sigma^2} e^{-\frac{\beta^2|Z_t|^2}{2\sigma^2}} \quad (28)$$

whereas the mean value and the variance (26)-(27) provide:

$$\mu_\beta \cong \frac{1}{|Z_t|}\mu_w \quad (29)$$

$$\sigma_\beta^2 \cong \frac{1}{|Z_t|^2}\sigma_w^2 \quad (30)$$

4 Numerical Validation

Analytical results derived in Section 3 have been validated through numerical simulations. In particular, the formulas (17) and (23) for the correlation coefficient, (18) for the PDF, and (26)-(27) for the mean value and the variance have been assessed against numerical simulations. Notice that the random variable *w* has been tested instead of β. Indeed, since $\beta = w/|Z_t|$ (see (13)), analytical results for β and for w are related in a straightforward way as shown by (28)-(30).

Numerical simulations were performed by selecting $\delta_a, \delta_b, \delta_c$ as uncorrelated zero-mean Gaussian random variables with standard deviations $\sigma_a, \sigma_b, \sigma_c$. The standard deviation σ_c was assumed as reference, with value $\sigma_c = 0.1$. Thus, the two ratios σ_a/σ_c and σ_b/σ_c were considered as parameters or variables. Repeated runs were performed (10^6 runs) to obtain the numerical estimate of each quantity to be validated (i.e., correlation coefficient, PDF, mean value and variance). In the following figures, numerical results from simulations are represented with dotted lines, whereas analytical results derived in Section 3 are represented with solid lines.

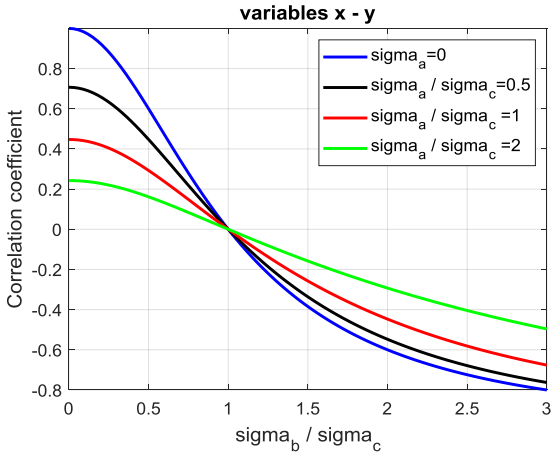

Fig. 4: Correlation coefficient (17) between variables *x* and *y* as defined in (15), as a function of σ_b/σ_c, for four different values of σ_a/σ_c. Numerical results (not visible in this figure) are perfectly overlapped by the solid lines corresponding to analytical results.

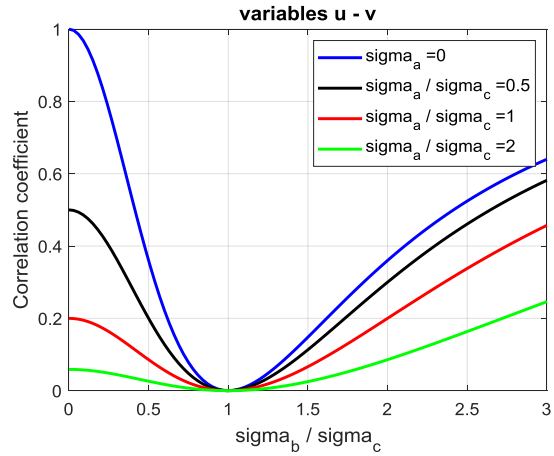

Fig. 5: Correlation coefficient (23) between variables u and v as defined before (20), as a function of σ_b/σ_c, for four different values of σ_a/σ_c. Numerical results (not visible in this figure) are perfectly overlapped by the solid lines corresponding to analytical results.

Fig. 4 shows the behavior of the correlation coefficient r_{xy}, given by (17), as a function of σ_b/σ_c by assuming σ_a/σ_c as a parameter. The solid lines corresponding to (17) overlap the dotted lines corresponding to numerical results. Therefore, dotted lines are not visible in Fig. 4. Notice that all the curves provide $r_{xy} = 0$ for $\sigma_b = \sigma_c$ as it was clearly shown by (17). Moreover, according to (15), correlation becomes negative as σ_b increases, and vice versa. From (15), it is also clear that by increasing σ_a correlation decreases because the random variable δ_a is involved only in the definition of *x*.

Fig. 5 shows the behavior of the correlation coefficient r_{uv}, given by (23), as a function of σ_b/σ_c, by assuming σ_a/σ_c as a parameter. As already mentioned $r_{uv} = r_{xy}^2$, thus Fig. 5 is strongly related to Fig. 4.

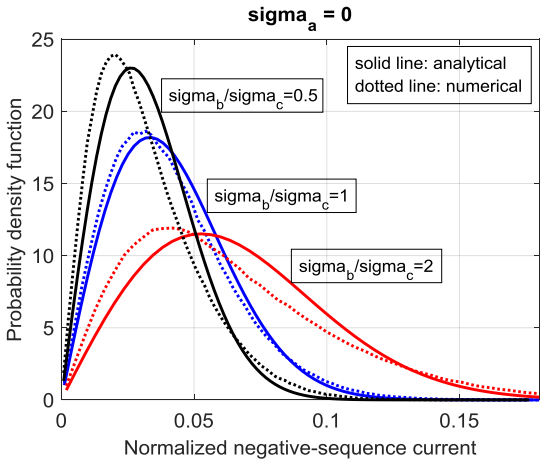

Fig. 6. Probability density function of the random variable w given by (20) for $\sigma_a = 0$ and three different values of σ_b/σ_c.

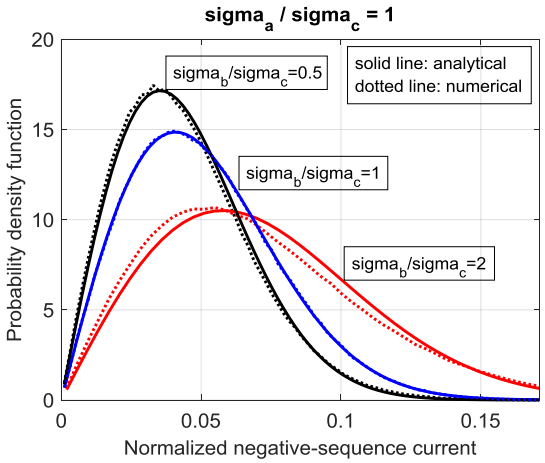

Fig. 7: Probability density function of the random variable w given by (20) for $\sigma_a = \sigma_c$ and three different values of σ_b/σ_c.

Indeed, the information about the sign of the correlation is lost, but from Fig. 5 the magnitude of the correlation coefficient allows a quantitative evaluation about the assumption of weakly correlated random variables. In fact, in case of weak correlation the random variable w given by (20) can be approximated by a Rayleigh random variable. This point is investigated in Fig. 6 where the PDF of w is reported in the case $\sigma_a = 0$. In Fig. 5 the curve for $\sigma_a = 0$ shows a wide excursion of the correlation coefficient which equals zero for $\sigma_b/\sigma_c = 1$, whereas it takes increasing values as σ_b/σ_c moves away from 1. In Fig. 6 three values were selected for σ_b/σ_c, i.e., 0.5, 1, 2. It can be noticed that for $\sigma_b/\sigma_c = 1$ the Rayleigh PDF (18) is a good approximation of the numerical PDF because the random variables u and v are uncorrelated. On the contrary, for $\sigma_b/\sigma_c = 0.5$ and $\sigma_b/\sigma_c = 2$ the strong correlation between u and v leads to a worse approximation of the Rayleigh PDFs to the numerical results. This is what we expected on the basis of the correlation coefficient in Fig. 5.

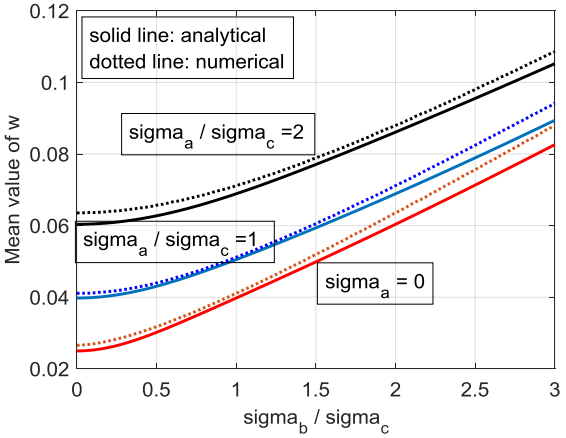

Fig. 8: Mean value of w, given by (26), as a function of σ_b/σ_c, for three different values of σ_a/σ_c, compared with numerical simulations.

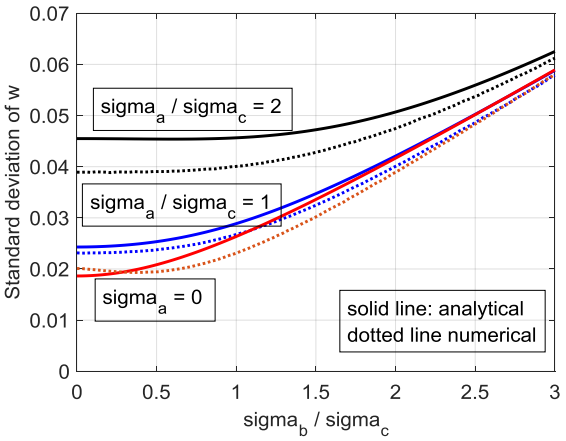

Fig. 9: Standard deviation of w, given by the square root of (27), as a function of σ_b/σ_c, for three different values of σ_a/σ_c, compared with numerical simulations.

Fig. 7 is similar to Fig. 6, but in this case $\sigma_a/\sigma_c = 1$ was assumed. From Fig. 5 we see that for $\sigma_a/\sigma_c = 1$ the correlation coefficient has a lower excursion. Therefore, we expect that the Rayleigh PDF is a better approximation to the numerical PDF with respect to Fig. 6. Moreover, we expect that for $\sigma_b/\sigma_c = 1$ we obtain the best approximation because in this case the correlation coefficient is

zero. This is confirmed by the three curves depicted in Fig. 7.

Fig. 8 shows the behavior of the mean value of w, given by (26), as a function of σ_b/σ_c, for three different values of σ_a/σ_c, compared with numerical simulations. The approximation provided by (26) is satisfactory, even if it always provides a slight underestimation with respect to numerical values.

Fig. 9 shows the behavior of the standard deviation of w, given by the square root of (27), as a function of σ_b/σ_c, for three different values of σ_a/σ_c, compared with numerical simulations. In this case, the approximation provided by (27) is less satisfactory with respect to the mean value approximation. The reason is likely due to the fact that the Taylor approximation (25) for the variance takes into account only the first derivatives, whereas the approximate mean value (24) takes into account the second derivatives. Nevertheless, the maximum error in Fig. 9 is lower than 20%.

Finally, the case where the random variables $\delta_a, \delta_b, \delta_c$ are uniform instead of Gaussian was investigated. Fig. 10 shows the behavior of the PDF of w by assuming uniform $\delta_a, \delta_b, \delta_c$ with $\sigma_a = \sigma_c$, and three different values for σ_b/σ_c. The figure should be compared with the analogous Fig. 7 where the same standard deviations were considered, but the underlying random variables $\delta_a, \delta_b, \delta_c$ were Gaussian. Notice that, contrary to Fig. 7, in Fig. 10 even the case $\sigma_b/\sigma_c = 1$ is deviating from the ideal Rayleigh behavior (solid line) because of the uniform instead of Gaussian distribution of $\delta_a, \delta_b, \delta_c$.

5 Conclusions

In the paper it was shown that by assuming Gaussian distribution for the parameters of an unbalanced three-phase component, the current injected in the negative-sequence circuit is approximately distributed as a Rayleigh variable. The degree of this approximation is strictly related to the correlation coefficients between the real and the imaginary parts of the injected current. Therefore, the evaluation of the correlation coefficient is crucial in the estimation of the accuracy of the Rayleigh distribution. Moreover, approximate expressions for the mean value and the variance of the injected current have been derived. The analytical result for the mean value is satisfactory, whereas the analytical results for the variance is affected by a larger error since only the first derivatives are retained in the Taylor expansion. Using higher order derivatives, however, would lead to much more complicated analytical expressions.

Future work will be devoted to extending the derivations to a more general unbalanced three-phase component instead of a simple resistive component. Moreover, different kinds of statistical distributions of the unbalanced component parameters will be considered beyond the Gaussian distribution. Future research will be also conducted in order to extend the proposed approach to typical power system loads characterized in terms of active and reactive power instead of impedance.

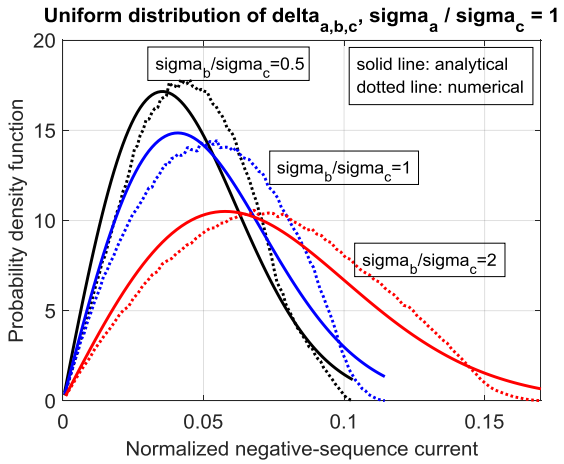

Fig. 10: Probability density function of the random variable w given by (20) for $\sigma_a = \sigma_c$ and three different values of σ_b/σ_c, assuming uniform distributions for $\delta_a, \delta_b, \delta_c$ instead of Gaussian as in Fig. 7.

References:

[1] C. L. Fortescue, Method of symmetrical coordinates applied to the solution of polyphase networks, *Trans. AIEE*, vol. 37, 1918, pp. 1027-1140.

[2] G. Chicco, P. Postolache, and C. Toader, Analysis of three-phase systems with neutral under distorted and unbalanced conditions in the symmetrical component-based framework, *IEEE Trans. on Power Delivery*, vol. 22, no.1, 2007, pp. 674-683.

[3] Cornelia A. Bulucea, Doru A. Nicola, Carmen A. Bulucea, Comprehensive Analysis Dedicated to Three-phase Power Transformer With Three-phase Bridge in AC/DC Traction Substations, *WSEAS Transactions on Systems and Control*, vol. 14, 2019, pp. 306-318.

[4] J. C. Das, *Understanding symmetrical components for power system modeling*. Piscataway, NJ: IEEE Press, 2017.

[5] D. Bellan, G. Superti Furga, and S. A. Pignari, Circuit representation of load and line

asymmetries in three-phase power systems, *International Journal of Circuits, Systems and Signal Processing*, vol. 9, 2015, pp. 75-80.

[6] *Electromagnetic compatibility (EMC) - limits - assessment of emission limits for the connection of unbalanced installations to MV, HV and EHV power systems*, Technical report IEC/TR 61000-3-13, Ed. I, International Electrotechnical Commission, 2008.

[7] D. Bellan and S. A. Pignari, Circuit representation of voltage unbalance emission due to line asymmetry, in *Proc. 2015 IEEE Innovative Smart Grid Technologies - Asia (ISGT ASIA)*, pp. 1-5.

[8] D. Bellan and S. A. Pignari, A circuit approach for the propagation analysis of voltage unbalance emission in power systems, in *Proc. 2016 IEEE PES Asia Pacific Power and Energy Engineering Conference (APPEEC 2016)*, pp. 1355-1359.

[9] R. Muzzammel and U. Tahir, Analytical behaviour of line asymmetries in three phase power systems, in Proc. of *IEEE International Symposium on Recent Advances in Electrical Engineering*, 24-26 October, 2017, Islamabad, Pakistan.

[10] J. Jayachandran and R. Murali Sachithanandam, Implementation of Neural Network Based I cos φ Controller for DSTATCOM in Three Phase Four Wire Distribution System Under Varying Source and Load Conditions for Power Quality Improvement, *WSEAS Transactions on Systems and Control*, vol. 11, 2016, pp. 199-216.

[11] T. Ahmadi, A Novel Multi Stage Transformer for Compensating Unbalanced Loads, *WSEAS Transactions on Systems and Control*, vol. 15, 2020, pp. 282-286.

[12] Z. Emin and D. S. Crisford, Negative phase-sequence voltages on E&W transmission system, *IEEE Trans. on Power Delivery*, vol. 21, no. 3, 2006, pp. 1607-1612.

[13] P. Paranavithana, S. Perera, R. Koch, and Z. Emin, Global voltage unbalance in MV networks due to line asymmetries, *IEEE Trans. on Power Delivery*, vol. 24, no. 4, 2009, pp. 2353-2360.

[14] Da Young Tu'uau, Timaima Marica, Mansour H. Assaf, Electric Power System Fault Analysis, *WSEAS Transactions on Circuits and Systems*, vol. 19, 2020, pp. 19-27.

[15] H. Renner, Voltage unbalance emission assessment, in *Proc. Elect. Power Quality Supply Reliability Conf.*, June 2010, pp. 43-48.

[16] U. Jayatunga, S. Perera, and P. Ciufo, Voltage unbalance emission assessment in radial power systems, *IEEE Trans. Power Delivery*, vol. 27, no. 3, 2012, pp. 1653-1661.

[17] U. Jayatunga, S. Perera, P. Ciufo, and A. P. Agalgaonkar, Deterministic methodologies for the quantification of voltage unbalance propagation in radial and interconnected networks, *IET Generation, Transmission & Distribution*, vol. 9, no. 11, 2015, pp. 1069-1076.

[18] M. Olofsson and U. Grape, Voltage quality in the context of EMC, in *Proc. 2009 International Symposium on Electromagnetic Compatibility*, Kyoto, Japan, pp. 241-244.

[19] D. Bellan, Approximate Circuit Representation of Voltage Unbalance Emission Due to Load Asymmetry in Three-Phase Power Systems, in *Proc. of the 4th IEEE Global Electromagnetic Compatibility Conference* (GEMCCON), Stellenbosch, South Africa, 7-9 November, 2018, pp. 1-4.

[20] D. Bellan, Statistical Analysis of Voltage Unbalance Emission Due to Asymmetrical Loads in Three-Phase Power Systems, *International Journal of Circuits, Systems and Signal Processing*, vol. 16, 2022, pp. 747-753.

[21] D. Bellan, Probability density function of three-phase ellipse parameters for the characterization of noisy voltage sags, *IEEE Access*, vol. 8, 2020, pp. 185503-185513.

[22] D. Bellan, Circuit modeling and statistical analysis of differential-to-common-mode noise conversion due to filter unbalancing in three-phase motor drive systems, *Electronics*, vol. 9, 2020, pp. 1-20.

[23] D. Bellan, Characteristic Function of Fundamental and Harmonic Active Power in Digital Measurements Under Nonsinusoidal Conditions, *International Review of Electrical Engineering*, vol. 10, no. 4, 2015, pp. 520-527.

[24] D. Bellan and S. A. Pignari, Estimation of crosstalk in nonuniform cable bundles, in *Proc. of 2005 IEEE International Symposium on Electromagnetic Compatibility*, USA, 8-12 Aug. 2005, pp. 336-341.